



A Journal of the Gesellschaft Deutscher Chemiker

Angewandte Chemie

GDCh

International Edition

www.angewandte.org

Accepted Article

Title: Ultra-Low Loading Pt/CeO₂ Catalysts: Ceria Facet Effect Affords Improved Pairwise Selectivity for Parahydrogen Enhanced NMR

Authors: Bochuan Song, Diana Choi, Yan Xin, Clifford R Bowers, and Helena Hagelin Weaver

This manuscript has been accepted after peer review and appears as an Accepted Article online prior to editing, proofing, and formal publication of the final Version of Record (VoR). This work is currently citable by using the Digital Object Identifier (DOI) given below. The VoR will be published online in Early View as soon as possible and may be different to this Accepted Article as a result of editing. Readers should obtain the VoR from the journal website shown below when it is published to ensure accuracy of information. The authors are responsible for the content of this Accepted Article.

To be cited as: *Angew. Chem. Int. Ed.* 10.1002/anie.202012469

Link to VoR: <https://doi.org/10.1002/anie.202012469>

Ultra-Low Loading Pt/CeO₂ Catalysts: Ceria Facet Effect Affords Improved Pairwise Selectivity for Parahydrogen Enhanced NMR

Bochuan Song,^[a] Diana Choi,^[b] Yan Xin,^[c] Clifford R. Bowers^{*[b]} and Helena Hagelin-Weaver^{*[a]}

[a] B. Song, Prof. H. E. Hagelin-Weaver
Department of Chemical Engineering
University of Florida
Gainesville, FL 32611 (USA)
E-mail: hweaver@che.ufl.edu

[b] D. Choi, Prof. C. R. Bowers
Department of Chemistry
University of Florida
Gainesville, FL 32611 (USA) University of Florida
E-mail: bowers@chem.ufl.edu
Gainesville, FL 32611 (USA)

[c] Y. Xin
National High Magnetic Field Laboratory
Florida State University
Tallahassee, FL 32310, USA

Supporting information for this article is given via a link at the end of the document.

Abstract: Oxide supports with well-defined shapes are beneficial in catalysis studies as they enable investigations on the effects of surface structure on metal-support interactions as well as correlations to catalytic activity and selectivity. Here, a modified atomic layer deposition technique was developed to achieve ultra-low loadings (8–16 ppm) of Pt on shaped ceria nanocrystals. By using octahedra and cubes, which expose exclusively (111) and (100) surfaces respectively, the effect of CeO₂ surface facet on the Pt-CeO₂ interactions under reducing conditions was revealed. Strong electronic interactions were found to result in electron-deficient Pt species on the CeO₂ (111) after reduction, which increased the stability of the atomically dispersed Pt and afforded significantly higher NMR signal enhancement compared with the electron-rich platinum on the CeO₂ (100), and a factor of two higher pairwise selectivity (6.1 %) than previously reported for a monometallic heterogeneous Pt catalyst.

Catalysts with atomically dispersed active metals have attracted significant attention as they afford maximum atomic efficiency, which is especially important when using precious metals such as Pt.^[1] While isolated Pt ions are remarkably stable under oxidative conditions on supports like CeO₂,^[2] improving stability under reducing conditions remains a challenge that must be addressed for hydrogenation reactions.^[3] We hypothesize that atomically dispersed Pt on a CeO₂ support (either as isolated Pt^{δ+} ions or Pt_x^{δ+} clusters interacting strongly with the CeO₂) can improve the pairwise selective addition of H₂ to unsaturated substrates, the latter a necessary property in parahydrogen-induced polarization (PHIP) Nuclear Magnetic Resonance (NMR) (*vide infra*). To limit Pt agglomeration to the greatest extent possible, we prepared ultra-low Pt loadings using a modified atomic layer deposition (ALD) process to maximize the distance between Pt atoms or ions. Furthermore, to investigate the dependence of the metal-support interactions on the surface facet exposed in Pt-CeO₂ catalysts,^[4] two different well-defined CeO₂ shapes were used as supports, namely, octahedra and cubes, which exclusively expose (111) and (100) surfaces, respectively. The resulting catalysts were

evaluated in the hydrogenation of propene, a standard probe reaction for characterizing the PHIP performance.

The Pt/CeO₂ catalysts were synthesized by carefully controlling the dose time (5 s) during ALD (see Supporting Information). At the same deposition temperature (180 °C), a smaller Pt loading is observed on the CeO₂ cubes compared with the octahedra, despite the slightly higher specific surface area of the cubes (Table 1). To match the Pt loadings and allow direct comparisons between the catalysts, a lower deposition temperature (120 °C) was also used for the CeO₂ octahedra (Table 1). The Pt loadings in this study (8–16 ppm) are an order of magnitude lower than previously reported ultra-low loading catalysts.^[5] Only isolated Pt ions are present on the (111) and (100) surfaces of the CeO₂ octahedra and cubes after deposition and a calcination treatment with static air at 350 °C (Figures 1c,f and S1), consistent with the stability of isolated Pt under oxidative conditions.^[2b, 3c] The surface Pt ions are located in the same positions as Ce ions since they coordinate to oxygen ions, either by replacing a cerium ion in the lattice or by bonding to the top of the oxygen-terminated CeO₂ surfaces.^[3a]

After temperature programmed reduction (TPR, Figure S2), the Pt species on the surfaces of the CeO₂ shapes have a very different appearance (Figures 1, S1), revealing a highly facet dependent stability under reducing conditions. While the isolated Pt atoms are essentially preserved on the CeO₂ octahedra, only Pt nanoparticles (no isolated Pt atoms) are present on the CeO₂ cubes after reduction (Figures 1d,g). Reduction of Pt²⁺ to Pt⁰ on CeO₂(100) is known to destabilize the Pt-CeO₂ interactions, and this is exacerbated by hydrogen spillover which results in CeO₂ reduction and facile migration of Pt across the CeO₂ (100) surface.^[3c, 4b] The CeO₂ (100) surface is easier to reduce than the CeO₂ (111) surface facet,^[6] which may account for the higher stability of Pt on CeO₂ (111). Additionally, strong electronic metal support interactions (EMSI) have also been observed for small Pt nanoparticles supported on CeO₂ (111) surfaces.^[7] The minimal

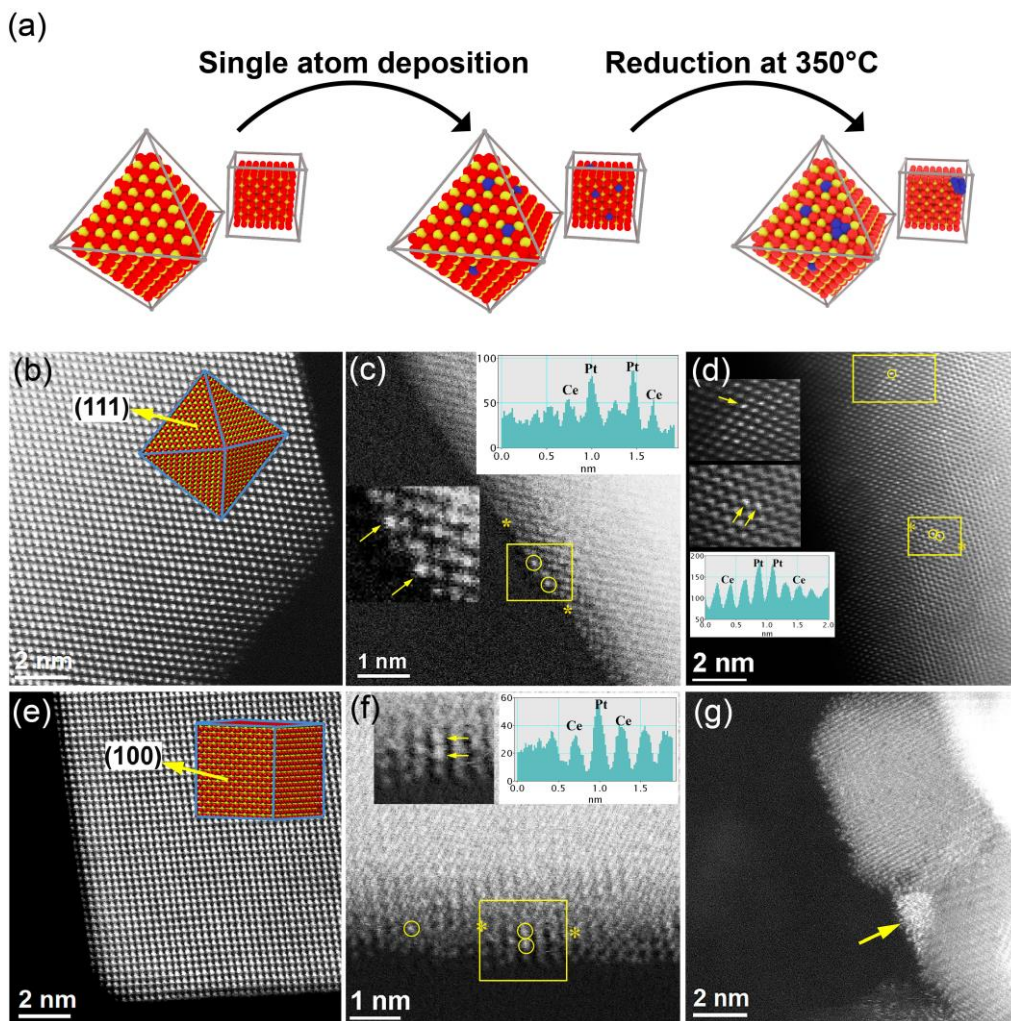


Figure 1. (a) Scheme of ultra-low loading catalysts on ceria octahedra and cubes synthesized via atomic layer deposition illustrating the different behavior of Pt following temperature programmed reduction (TPR) to 350 °C before PHIP experiments. The high angle annular dark field scanning transmission electron microscopy (HAADF-STEM) images of the catalysts after calcination reveal very well defined CeO₂ surface facets, the expected (111) for the octahedra (b) and (100) for the cubes (e). High-resolution STEM images of fresh (c) Oct-16ppm and (f) Cub-10ppm catalysts reveal only isolated Pt ions after the calcination treatment. After temperature programmed reduction (TPR) the Oct-16ppm catalyst (d) still reveal visible isolated Pt. The Cub-10ppm catalyst after TPR (g) in contrast contains exclusively Pt nanoparticles (as indicated by the yellow arrow). Yellow circles in (c), (d) and (f) indicate individual Pt atoms and insets display the line intensity profile along the line between the two * symbols.

formation of small flat Pt clusters (Figure S3) on the octahedra further supports the presence of strong interactions with the CeO₂ (111) facet. Such EMSI have been shown to increase the pairwise selectivity in hydrogenation reactions.^[8]

PHIP^[9] is a technique for generating nuclear-spin-hyperpolarized fluids for sensitivity enhancement of NMR and MRI signals. Compared to the dynamic nuclear polarization method, parahydrogen based techniques use relatively uncomplicated instrumentation with lower cost and shorter polarization times.^[10] A key advantage of heterogeneous hydrogenation over supported metals is the facile separation of the solid catalysts from the

Table 1. Properties of Pt catalysts supported on CeO₂ octahedra (Oct) and cubes (Cub). Support surface facet and specific surface area, Pt loading, and ALD deposition temperature of ultra-low loading catalysts.

Catalyst ^[a]	Surface Facet	Surface area [m ² /g]	Pt loading [ppm] ^(a)	ALD temperature [°C]
Oct-8ppm	111	13.7±1.4	8.2	120
Cub-10ppm	100	18.4±0.7	10	180
Oct-16ppm	111	13.7±1.4	16	180

[a] 1 ppm equals 1 mg Pt metal over 1 kg CeO₂, so that 10 ppm = 0.001 wt%. ICP-MS on a duplicate Oct-8ppm sample confirms reproducibility (Table S1).

hyperpolarized gas or liquid phase products.^[11] Unfortunately, these catalysts exhibit a low pairwise selectivity of parahydrogen addition to unsaturated substrates. The low pairwise selectivity, and thus low NMR signal enhancement, is due to a combination of (i) the high mobility of hydrogen atoms after facile dissociation on metal surfaces and (ii) the step-wise addition of hydrogen to the substrate in the Horiuti–Polanyi mechanism leading to a loss of the singlet spin order of parahydrogen.^[10c] To test our hypothesis that atomically dispersed Pt/CeO₂ catalysts can improve the pairwise selectivity, continuous-flow propene hydrogenation reactions were conducted with either 50% enriched parahydrogen (p-H₂) or normal hydrogen (n-H₂). The PHIP NMR spectra (Figure 2), collected in ALTADENA mode,^[8] reveal that a reaction temperature of 200 °C is necessary to observe significant activity and pairwise selectivity (Figures 3, S4-S6). Under the reducing conditions used in this study, neither the bare CeO₂ octahedra nor the cubes contribute to the reactivity, as shown in Figures 3, S7.^[12]

As expected, the higher the Pt content of these catalysts, the higher the propene conversion (more active sites), but despite the ultra-low Pt content, the pairwise selectivity is low. The PHIP signal enhancement over these catalysts may be limited by the randomization of the parahydrogen singlet state accompanying hydrogen spillover from Pt to CeO₂,^[13] rather than by the rapid hydrogen diffusion observed on larger Pt particles.^[14] In all cases, the pairwise selectivity is higher at a reaction temperature of

300 °C compared with 200 °C, indicating that the rate of hydrogen addition to propene increases faster than the spillover rate (or the rate of surface hydrogen diffusion on the Pt metal particles on the CeO₂ cube support). The propene conversion over the Oct-8ppm catalyst also increases, resulting in an intense PHIP signal (Figure 2). The pairwise selectivity of 6.1 % obtained over the Oct-8ppm catalyst is significantly higher than the 0.3-0.4 % obtained over a conventionally prepared Pt/TiO₂ catalyst run under similar conditions (Figure S8). Amongst monometallic heterogeneous catalysts, only supported Rh, a metal known to give higher pairwise selectivities than Pt, has yielded a similar pairwise selectivity in the hydrogenation of propene.^[15]

A lower pairwise selectivity (2.7 %) is observed over the Cub-10ppm catalyst which displayed Pt nanoparticle formation, but this is still significantly higher than that obtained with the conventional Pt/TiO₂ catalyst under the same conditions, and it is comparable to the best supported Pt catalyst in the literature.^[14] Furthermore, the reaction rates normalized by Pt content of the catalysts in this study are several orders of magnitude higher than those of the Pt/TiO₂ catalyst (Figure 3c), which means that the Pt is utilized very efficiently in these ultra-low loading catalysts. The loss in activity and increase in selectivity observed on the Cub-10ppm and Oct-16ppm between 200 and 300 °C are inconsistent with sintering (Pt particle growth).^[14] The observed behavior could be explained by carbon deposition (coking) under the propene-rich reaction conditions, as the carbon would block active sites and hinder hydrogen diffusion. However, there was no indication of significant coking during these experiments (Figure S9). A more likely explanation for the decreased conversion and increased pairwise selectivity at the higher temperature is the induction of EMSI, as has been previously reported on other reducible supports.^[8] The higher activity of the Oct-8ppm catalyst at 300 versus 200 °C may suggest that the flat clusters, which we observed in the TEM of the Oct-8ppm catalyst following the reaction studies (Figure S10), are more active in the hydrogenation reaction than the isolated Pt ions on the octahedra.

To investigate the nature of the Pt-CeO₂ interactions on these catalysts, diffuse reflectance infrared Fourier transform spectroscopy (DRIFTS) was performed on the reduced Pt/CeO₂ catalysts after CO adsorption at room temperature. Three distinct features are observed in IR spectra obtained from Pt supported

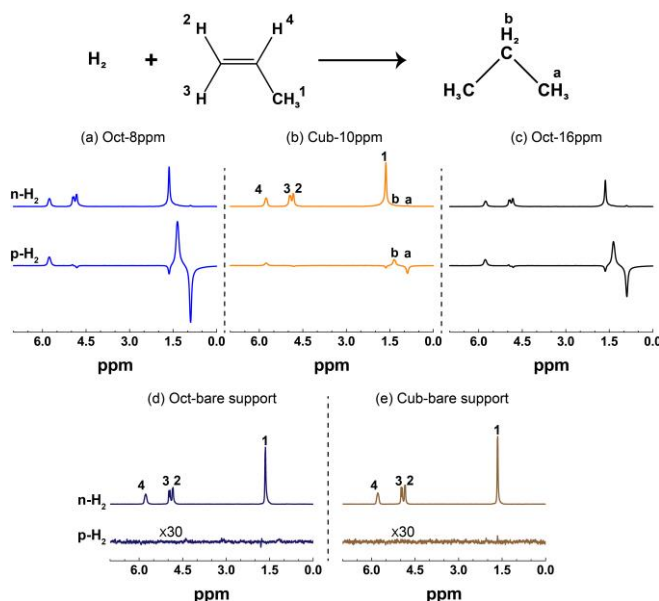


Figure 2. Thermally polarized (*n*-H₂ top) and hyperpolarized (*p*-H₂, bottom) ¹H NMR spectra collected with 10mg of (a) Oct-8ppm, (b) Cub-10ppm, (c) Oct-16ppm, (d) bare octahedra and (e) bare cubes at 300 °C. The flow rates were 365/30/105 mL/min N₂/H₂/propene. All spectra are shown at the same scale.

on the CeO₂ octahedra (Figure 4). Unambiguous assignment of the DRIFTS peaks is challenging, but the peak near 2105 cm⁻¹ is due to strongly bound CO on electron poor Pt,^[2a, 16] and has previously been assigned to isolated Pt^{δ+} ions,^[5b, 16] or PtO_x clusters.^[17] This is consistent with a weak peak above 2100 cm⁻¹ being the main feature in the spectra obtained from the fresh (unreduced) catalyst (see Figure S11). CO DRIFTS peaks at 2075 cm⁻¹ are typically assigned to nm-size Pt particles,^[3b, 17a] but no particles of this size are observed on the ceria octahedra. It is possible that a small electron-deficient Pt cluster could result in CO DRIFTS peaks at the same wavenumber. However, calculations indicate that CO adsorbed on single atom Pt (i.e. Pt⁰) on CeO₂(111) surface facets would exhibit a peak at 2075 cm⁻¹.^[17b] Experimentally, isolated Pt atoms, i.e. Pt⁰, have not been observed at this wavenumber for Pt/CeO₂ catalysts, which could be because they are difficult to generate and require CeO₂ octahedra with exclusive (111) surface facets. Isolated Pt ions

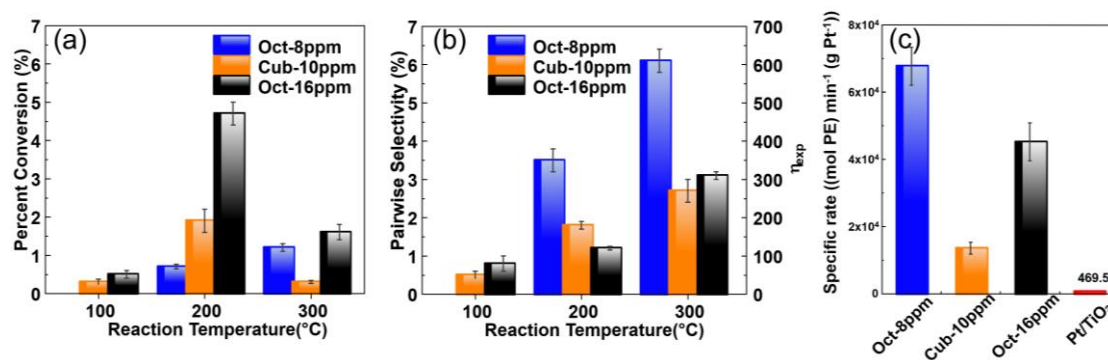


Figure 3. Temperature dependence of (a) propene conversion and (b) pairwise selectivity and corresponding η_{exp} (signal enhancement) in the hydrogenation of propene to propane over Pt supported on CeO₂ shapes determined using PHIP NMR spectra. The flow rates were 365/30/105 mL/min N₂/H₂/propene. (c) Reaction rate of propene hydrogenation at 300 °C per unit weight of Pt over the ultra-low loading Pt/CeO₂ catalysts and a reference Pt/TiO₂ catalyst with a 0.76% Pt loading synthesized via precipitation. Reactant flow rates are the same as in (a) and (b).

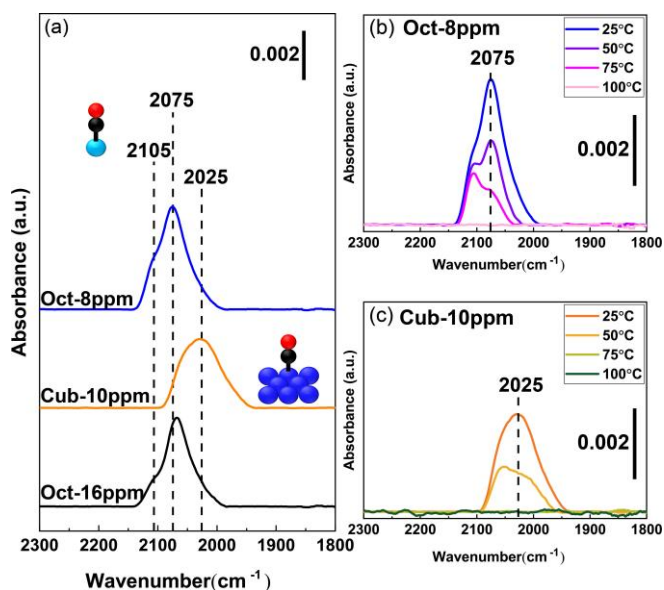


Figure 4. CO DRIFTS (diffuse reflectance infrared Fourier transform spectroscopy) data obtained from (a) Oct-8ppm, Cub-10ppm and Oct-16ppm and after reduction in H₂ (5% in N₂) at 350 °C and a CO exposure at 25 °C. Data collected after desorption of CO in a flow of He at 25, 50, 75, and 100 °C are shown for Oct-8ppm (b) and Cub-10ppm CO (c).

(Pt²⁺) on conventional CeO₂ supports bind very strongly at defects or step edges (sites that are not present on the CeO₂ octahedra), and reduction of these ions therefore requires reduction temperatures above 400 °C.^[3a, 18] At these temperatures the Pt atoms are unstable and highly mobile on the support, which results in agglomeration and formation of Pt nanoparticles. The temperature programmed desorption profile (Figure 4b) reveals no redshift in the IR peaks, and thus a lack of dipole-dipole coupling between CO molecules on the octahedra-supported catalysts, and this further supports the assignment of the most intense IR peak to isolated atoms and it is also consistent with Pt atoms being the majority species in the STEM data.^[16] A small shoulder due to a peak around 2050 cm⁻¹ is also present, which is likely due to CO adsorbed on trace amounts of Pt nanoparticles.^[19]

In contrast, CO adsorbed on the Cub-10ppm catalyst yields two features at low wavenumber, likely due to metallic Pt particles of different sizes,^[20] or potentially Pt in different locations on the CeO₂ cubes. The 2050 cm⁻¹ peak is consistent with previous reported CO adsorbed on small Pt particles on ceria support.^[21] The more intense feature at 2025 cm⁻¹ is due to electron-rich Pt particles, likely as a result of weaker interactions with the CeO₂ cubes. The absence of peaks at higher wave number (>2070 cm⁻¹) on the Cub-10ppm catalyst is consistent with the lack of visible isolated Pt atoms on this support (Figure 1g).

The DRIFTS data illustrate the difference in electron density of Pt on the two CeO₂ surface facets. EMSI results in electron-poor Pt species on the CeO₂ (111) surfaces of the octahedra, which stabilizes isolated Pt against severe sintering (only a few small Pt clusters are formed). In contrast, reducing conditions destabilize the Pt-CeO₂ interactions on the CeO₂ (100) surfaces of the cubes and, despite the ultra-low loading, larger electron-rich Pt nanoparticle are formed. The observation of higher PHIP signals for the electron-poor catalyst supports our hypothesis that

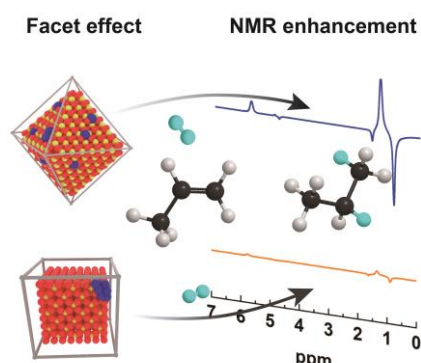
atomically dispersed Pt^{δ+} on a CeO₂ support can yield a higher pairwise selectivity. This is likely due to a combined size and electronic effect, which together with the high turnover frequency, indicate that atomically dispersed catalysts have outstanding potential as atom-efficient catalysts for parahydrogen induced polarization. Such catalysts afford cost-effective scaling-up of continuous-flow hetPHIP, which is important for applications (e.g. sensitivity-enhanced medical MRI) requiring large quantities of hyperpolarized gases.

Acknowledgements

Funding for this work was provided by NSF CHE-1507230 and CBET-1933723, and the National High Magnetic Field Laboratory, which is supported by the NSF Cooperative Agreement DMR-1644779 and the State of Florida. Funding from the University of Florida is also gratefully acknowledged.

Keywords: Ceria nanoshapes • Platinum • Hyperpolarization
NMR spectroscopy • Atomic layer deposition • Ultra-low loading

Entry for the Table of Contents



Stronger interactions are observed between Pt and the (111) surface facets of the CeO₂ octahedra compared with the (100) surfaces of the CeO₂ cubes. These interactions result in more stable and electron-poor Pt species on the CeO₂ octahedra, which translates to higher pairwise selective addition of parahydrogen to propene and enhanced NMR signals compared with the electron-rich nanoparticle Pt on the CeO₂ cubes.

Reference List

- [1] a) A. Wang, J. Li, T. Zhang, *Nature Reviews Chemistry* **2018**, *2*, 65-81; b) J. Li, Q. Guan, H. Wu, W. Liu, Y. Lin, Z. Sun, X. Ye, X. Zheng, H. Pan, J. Zhu, S. Chen, W. Zhang, S. Wei, J. Lu, *Journal of the American Chemical Society* **2019**; c) M. Yang, L. F. Allard, M. Flytzani-Stephanopoulos, *Journal of the American Chemical Society* **2013**, *135*, 3768-3771.
- [2] a) L. Nie, D. Mei, H. Xiong, B. Peng, Z. Ren, X. I. P. Hernandez, A. DeLaRiva, M. Wang, M. H. Engelhard, L. Kovarik, A. K. Datye, Y. Wang, *Science* **2017**, *358*, 1419; b) J. Jones, H. Xiong, A. T. DeLaRiva, E. J. Peterson, H. Pham, S. R. Challa, G. Qi, S. Oh, M. H. Wiebenga, X. I. Pereira Hernández, Y. Wang, A. K. Datye, *Science* **2016**, *353*, 150-154.
- [3] a) J. Resasco, L. DeRita, S. Dai, J. P. Chada, M. Xu, X. Yan, J. Finzel, S. Hanukovich, A. S. Hoffman, G. W. Graham, S. R. Bare, X. Pan, P. Christopher, *Journal of the American Chemical Society* **2020**, *142*, 169-184; b) X. Ye, H. Wang, Y. Lin, X. Liu, L. Cao, J. Gu, J. Lu, *Nano Res* **2019**; c) A. Bruix, Y. Lykhach, I. Matolinova, A. Neitzel, T. Skala, N. Tsud, M. Vorokhta, V. Stetsovych, K. Sevcikova, J. Myslivecek, R. Fiala, M. Vaclavu, K. C. Prince, S. Bruyere, V. Potin, F. Illas, V. Matolin, J. Libuda, K. M. Neyman, *Angew Chem Int Edit* **2014**, *53*, 10525-10530.
- [4] a) H. A. Aleksandrov, K. M. Neyman, G. N. Vayssilov, *Phys Chem Chem Phys* **2015**, *17*, 14551-14560; b) A. Bruix, K. M. Neyman, F. Illas, *J Phys Chem C* **2010**, *114*, 14202-14207; c) F. Dvorak, M. F. Camellone, A. Tovt, N. D. Tran, F. R. Negreiros, M. Vorokhta, T. Skala, I. Matolinova, J. Myslivecek, V. Matolin, S. Fabris, *Nature communications* **2016**, *7*, 8.
- [5] a) J. S. King, A. Wittstock, J. Biener, S. O. Kucheyev, Y. M. Wang, T. F. Baumann, S. K. Giri, A. V. Hamza, M. Baeumer, S. F. Bent, *Nano Letters* **2008**, *8*, 2405-2409; b) L. DeRita, S. Dai, K. Lopez-Zepeda, N. Pham, G. W. Graham, X. Pan, P. Christopher, *Journal of the American Chemical Society* **2017**, *139*, 14150-14165.
- [6] Z. Wu, M. Li, J. Howe, H. M. Meyer, 3rd, S. H. Overbury, *Langmuir* **2010**, *26*, 16595-16606.
- [7] a) S. D. Senanayake, J. A. Rodriguez, D. Stacchiola, *Topics in Catalysis* **2013**, *56*, 1488-1498; b) A. Bruix, A. Migani, G. N. Vayssilov, K. M. Neyman, J. Libuda, F. Illas, *Phys Chem Chem Phys* **2011**, *13*, 11384-11392.
- [8] E. W. Zhao, H. Zheng, K. Ludden, Y. Xin, H. E. Hagelin-Weaver, C. R. Bowers, *ACS Catalysis* **2016**, *6*, 974-978.
- [9] a) C. R. Bowers, D. P. Weitekamp, *Phys Rev Lett* **1986**, *57*, 2645-2648; b) C. R. Bowers, D. P. Weitekamp, *Journal of the American Chemical Society* **1987**, *109*, 5541-5542; c) T. C. Eisenschmid, R. U. Kirss, P. P. Deutsch, S. I. Hommeltoft, R. Eisenberg, J. Bargon, R. G. Lawler, A. L. Balch, *Journal of the American Chemical Society* **1987**, *109*, 8089-8091.
- [10] a) J. B. Hovener, A. N. Pravdivtsev, B. Kidd, C. R. Bowers, S. Glogglar, K. V. Kovtunov, M. Plaumann, R. Katz-Brull, K. Buckenmaier, A. Jerschow, F. Reineri, T. Theis, R. V. Shchepin, S. Wagner, P. Bhattacharya, N. M. Zacharias, E. Y. Chekmenev, *Angewandte Chemie* **2018**, *57*, 11140-11162; b) A. B. Schmidt, S. Berner, W. Schimpf, C. Muller, T. Lickert, N. Schwaderlapp, S. Knecht, J. G. Skinner, A. Dost, P. Rovedo, J. Hennig, D. von Elverfeldt, J. B. Hovener, *Nature communications* **2017**, *8*, 14535; c) R. Zhou, E. W. Zhao, W. Cheng, L. M. Neal, H. Zheng, R. E. Quinones, H. E. Hagelin-Weaver, C. R. Bowers, *Journal of the American Chemical Society* **2015**, *137*, 1938-1946.
- [11] a) K. V. Kovtunov, I. E. Beck, V. I. Bukhtiyarov, I. V. Koptuyug, *Angew Chem Int Edit* **2008**, *47*, 1492-1495; b) E. V. Pokochueva, K. V. Kovtunov, O. G. Salnikov, M. E. Gemeinhardt, L. M. Kovtunova, V. I. Bukhtiyarov, E. Y. Chekmenev, B. M. Goodson, I. V. Koptuyug, *PCCP* **2019**, *21*, 26477-26482.
- [12] a) E. W. Zhao, Y. Xin, H. E. Hagelin-Weaver, C. R. Bowers, *Chemcatchem* **2016**, *8*, 2197-2201; b) E. W. Zhao, H. Zheng, R. Zhou, H. E. Hagelin-Weaver, C. R. Bowers, *Angewandte Chemie* **2015**, *54*, 14270-14275.
- [13] G. Dutta, U. V. Waghmare, T. Baidya, M. S. Hegde, *Chemistry of Materials* **2007**, *19*, 6430-6436.
- [14] V. V. Zhivonitko, K. V. Kovtunov, I. E. Beck, A. B. Ayupov, V. I. Bukhtiyarov, I. V. Koptuyug, *The Journal of Physical Chemistry C* **2011**, *115*, 13386-13391.
- [15] E. Pokochueva, D. Burueva, L. Kovtunova, A. Bukhtiyarov, A. Gladky, K. V. Kovtunov, I. V. Koptuyug, V. Bukhtiyarov, *Faraday Discussions* **2020**.
- [16] K. Ding, A. Gulec, A. M. Johnson, N. M. Schweitzer, G. D. Stucky, L. D. Marks, P. C. Stair, *Science* **2015**, *350*, 189-192.
- [17] a) J. Ke, W. Zhu, Y. Jiang, R. Si, Y.-J. Wang, S.-C. Li, C. Jin, H. Liu, W.-G. Song, C.-H. Yan, Y.-W. Zhang, *ACS Catalysis* **2015**, *5*, 5164-5173; b) H. Wang, J. X. Liu, L. F.

COMMUNICATION

WILEY-VCH

- [18] Allard, S. Lee, J. Liu, H. Li, J. Wang, J. Wang, S. H. Oh, W. Li, M. Flytzani-Stephanopoulos, M. Shen, B. R. Goldsmith, M. Yang, *Nature communications* **2019**, *10*, 3808.
- [19] S. Zhang, L. Chen, Z. Qi, L. Zhuo, J. L. Chen, C. W. Pao, J. Su, G. A. Somorjai, *Journal of the American Chemical Society* **2020**, *142*, 16533-16537.
- [19] P. Bazin, O. Saur, J. C. Lavalley, M. Daturi, G. Blanchard, *Phys Chem Chem Phys* **2005**, *7*.
- [20] L. C. deMenorval, A. Chaqroune, B. Coq, F. Figueras, *J Chem Soc Faraday T* **1997**, *93*, 3715-3720.
- [21] a) W. Q. Xu, R. Si, S. D. Senanayake, J. Llorca, H. Idriss, D. Stacchiola, J. C. Hanson, J. A. Rodriguez, *Journal of Catalysis* **2012**, *291*, 117-126; b) C. M. Kalamaras, I. D. Gonzalez, R. M. Navarro, J. L. G. Fierro, A. M. Efstathiou, *J Phys Chem C* **2011**, *115*, 11595-11610.

WILEY-VCH

Accepted Manuscript